*J Mater Sci* (2019) 54:11179–11196

Materials for life sciences

# Immobilization via polydopamine of dual growth factors on polyetheretherketone: improvement of cell adhesion, proliferation, and osteo-differentiation

Teng Wan[1,2], Linlong Li[2,3], Min Guo[2], Zixue Jiao[2], Zongliang Wang[2], Yoshihiro Ito[4,5], Yizao Wan[6], Peibiao Zhang[2,3,*], and Qinyi Liu[1,*]

[1] *Department of Orthopaedics, The Second Hospital, Jilin University, Changchun 130041, People's Republic of China*
[2] *Key Laboratory of Polymer Ecomaterials, Changchun Institute of Applied Chemistry, Chinese Academy of Sciences, Changchun 130022, People's Republic of China*
[3] *University of Chinese Academy of Sciences, Beijing 100039, People's Republic of China*
[4] *Nano Medical Engineering Laboratory, RIKEN Center for Emergent Matter Science, RIKEN, 2-1 Hirosawa, Wako, Saitama 351-0198, Japan*
[5] *Emergent Bioengineering Materials Research Team, RIKEN Center for Emergent Matter Science, RIKEN, 2-1 Hirosawa, Wako, Saitama 351-0198, Japan*
[6] *Institute of Advanced Materials, East China Jiaotong University, 808 East Shuanggang Street, Nanchang, Jiangxi 330013, People's Republic of China*

**Received:** 20 August 2018
**Accepted:** 14 December 2018
**Published online:** 10 May 2019



## ABSTRACT

Polyetheretherketone (PEEK) is a promising biomedical material for orthopedic and dental applications owing to its excellent mechanical properties, near absence of immune toxicity, and X-radiolucency but suffers from bioinertness and inferior osteo-conduction. Surface modification of PEEK can effectively overcome these problems, while retaining most of its advantageous properties. In this study, the dual growth factors IGF-1 and BMP-2 were immobilized onto the porous surface of PEEK materials using polydopamine (pDA) coating to construct a bioactive interface. The surface characteristics of modified PEEK were evaluated by scanning electron microscopy and X-ray photoelectron spectroscopy. The pore size, generally distributed between 0.24 and 0.74 μm, was evaluated using ImageJ software. Hydrophilicity and BSA protein adsorption capacity were significantly enhanced after pDA coating. IGF-1 and BMP-2 were successfully immobilized onto the porous surface via pDA coating, and the immobilization efficiency was determined by ELISA. In vitro, samples treated with 50 ng/ml IGF-1 and 50 ng/ml BMP-2 showed better cytocompatibility for cell proliferation. The in vitro studies revealed that PEEK immobilized with dual growth factors could significantly improve cell attachment, spreading, proliferation, extracellular matrix secretion, alkaline phosphatase activity, and mineralization of MC3T3-E1 cells.

Address correspondence to E-mail: zhangpb@ciac.ac.cn; 1226527208@qq.com

https://doi.org/10.1007/s10853-018-03264-z

## Introduction

Orthopedic implants are hard tissue substitutes used as bone defect scaffolds, bone screws, interbody fusion cages, and so on [1]. Traditional metallic implants made of titanium alloys have been widely used as orthopedic implants for several decades owing to their excellent corrosion resistance, high mechanical strength, and biocompatibility [2]. However, release of harmful metal ions and a mismatched elastic modulus between the metal and cortical bone may lead to implant failure [3]; this has attracted the attention of many surgeons. Polyetheretherketone (PEEK) is a promising, alternative, polymeric material that has been widely used in the clinic owing to its excellent properties such as a low elastic modulus, which is close to that of human bone, high mechanical properties, near absence of immune toxicity, and X-radiolucency [4]. However, the surface bioinertness and inferior osseointegration of PEEK prevent a satisfactory biological interaction between the implant and surrounding bone tissue, thus limiting its further use in clinical applications [5].

Currently, many strategies are being studied to overcome the bioinert character of PEEK. One of the most important approaches is surface modification for the biofunctionalization of PEEK through surface treatment alone or in combination with surface coating [6–8]. Surface modification offers an effective way to increase the bioactivity of PEEK, while preserving most of its advantageous properties. Multiple studies have demonstrated [7, 9, 10] that the surface properties of biomaterials play a crucial role in cell–implant interactions at the implant/tissue interface during the bone healing process. In several studies [11], a surface porous structure has been fabricated on PEEK materials using concentrated sulfuric acid, and the results have shown that biocompatibility and osseointegration of PEEK could be improved to a certain extent by the three-dimensional porous structure.

In recent years, mussel-inspired polydopamine (pDA) surface modification has attracted much more interest than other surface modification methods because pDA surface modification is more convenient and easily operated [12, 13]. Moreover, pDA biomedical surface modification can provide the substrate material with many biocompatibility characteristics such as hydrophilicity, cell attachment, and proliferation of pre-osteoblasts [14, 15]. Furthermore, pDA layers possess many functional groups that can improve the bonding ability of substrates with biomolecules such as peptides, growth factors, and enzymes [16]. Chen et al. [17] showed that pDA coating could effectively immobilize growth factors on the sample surface and effectively reduce the burst release of growth factors to a sustained release rate compared to that obtained with physical absorption. Therefore, surface modification via pDA is an effective strategy to immobilize growth factors on the surface of polymer materials. Lastly, pDA could also improve the mineralization ability of substrates because of its capacity to attract calcium ions [18].

Growth factors play an important role in the bone healing process by allowing migration, adhesion, and proliferation of progenitor cells at the injury area [19], thus accelerating the bone healing process. Bone morphogenetic proteins (BMPs) are a key factor with significant osteogenic potential and promote bone regeneration [20]. A number of studies [19, 21, 22] have shown that BMP-2 can improve the expression of osteoblast functional proteins, increase alkaline phosphatase (ALP) activity, enhance the formation of mineralized nodules in vitro along with in vivo osteogenic potential. However, an inadequate cell proliferation capacity has restricted the biomedical applications of BMP-2 [23], indicating that the osseointegration ability of BMP-2 alone is unsatisfactory and could cause failure of internal implants and the surrounding bone tissue integration. The strategy used by many studies to improve the regenerative potential of BMP-based tissue engineering implants is to combine BMP-2 with other cytokines to enhance osteogenic capability and proliferation [24, 25]. Consequently, insulin-like growth factor-1(IGF-1), a growth-promoting cytokine that plays an important role in development, metabolism, and growth, has been considered a desirable candidate molecule to improve the BMP-based system in bone regenerative medicine [26]. Several studies have reported that combined release of BMP-2 and IGF-1 could induce higher osteogenic differentiation compared to the release of BMP-2 or IGF-1 alone [27, 28], indicating that combination of IGF-1 and BMP-2

could accelerate the bone healing process. Therefore, in present study, we decorated the PEEK surface with IGF-1 and BMP-2 in order to obtain better biological activity.

As shown in Fig. 1, in this study, dual growth factors IGF-1 and BMP-2 were immobilized onto the porous structure through an intermediate layer of pDA to construct a bioactive interface on PEEK materials. The surface morphological characteristics and wettability were investigated. Protein adsorption capacity was examined, and the immobilized IGF-1 and BMP-2 were quantified using ELISA. Furthermore, in order to evaluate the bioactivity of dual growth factor-loaded samples compared to single growth factor-loaded samples, we performed a series of in vitro tests for cell adhesion, spreading, proliferation, extracellular matrix secretion, and osteo-differentiation of MC3T3-E1 cells.

## Experimental section

### Materials

The PEEK used in this study was of medical grade (Victrex, England). Square samples of 1 cm × 1 cm × 0.02 cm size were prepared for the surface characterization, and disk samples with a diameter of 1.56 cm and a thickness of 0.02 cm were used for in vitro assessment in 24-well tissue culture plates. Recombinant human IGF-1 and BMP-2 were purchased from UB Biotech. Co. Ltd. Tris (hydroxymethyl), dopamine hydrochloride, p-nitrophenyl phosphate (PNPP), Alizarin Red-S, DAPI, and CCK-8 were purchased from Sigma-Aldrich (St. Louis, MO, USA). Human BMP-2 and IGF-1 ELISA kit was purchased from R&D Co.

### Preparation of surface porous structure

To obtain a relatively uniform porous structure, PEEK samples were immersed in concentrated sulfuric acid (95–98%) for 10 s with supersonic stirring at 25 °C. Afterward, the samples were taken out and immersed in supersonically stirred distilled water and rinsed repeatedly with distilled water. The samples were then dried at room temperature and referred as PEEK-P.

### Polydopamine coating and growth factor immobilization

The pDA coating process was performed as described previously [29]. Briefly, samples were placed in 24-well tissue culture plates, and 1 ml of pDA solution (2 mg/ml in 10 mM tris–HCL, pH = 8.5) was added to each well with a table concentrator at 37 °C for 4 h. The pDA-coated PEEK was then transferred to new 24-well tissue culture plates, followed by washing thrice with deionized water to remove the un-conglutinated pDA.

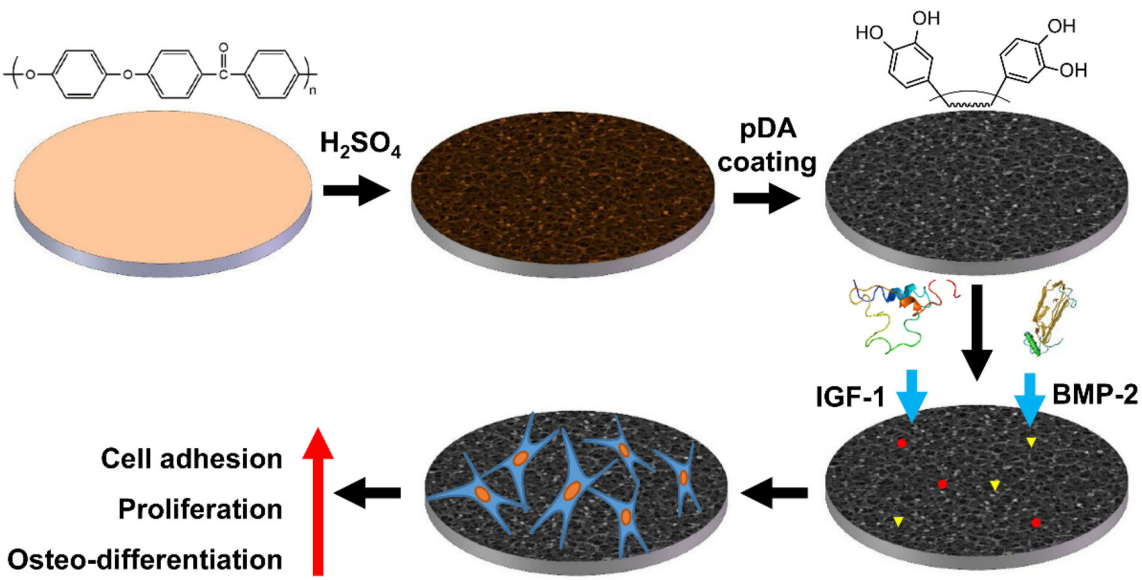


**Figure 1** Schematic diagram of the preparation and in vitro evaluation of the IGF-1/BMP-2 decorated porous surface PEEK films.

Next, 1 ml of IGF-1 (10 ng/ml, 50 ng/ml, and 100 ng/ml) or BMP-2 (10 ng/ml, 50 ng/ml, and 100 ng/ml) solution was added to each well and placed at 4 °C for 12 h. For the combined IGF-1 and BMP-2 group, 50 ng IGF-1 and 50 ng BMP-2 were both included in each milliliter of growth factor solution. The growth factor-loaded samples are hereafter named as "PEEK-P/pDA/IGF1, -1, -2, and -3," and "PEEK-P/pDA/BMP2 -1, -2, and -3," respectively, representing treatment with concentrations of 10 ng/ml, 50 ng/ml, and 100 ng/ml for IGF-1 or BMP-2 solutions. "PEEK-P/pDA/IGF1-BMP2" represents the dual growth factors, IGF-1 and BMP-2 (50 ng/ml IGF-1 and 50 ng/ml BMP-2). All the prepared samples and their abbreviations are summarized in Table 1.

## Surface characterization

The surface structure and pore size of the prepared specimens were observed using scanning electron microscopy (SEM) (XL30, Philips). To calculate the pore size on the surface of the treated layer, 200 pores were measured using ImageJ software. X-ray photoelectron spectroscopy (XPS) (Thermo) was employed to determine the elemental composition and chemical changes. Surface hydrophilicity of the specimens was assessed by water contact angle measurements (VCA 2000, AST).

## Adsorption kinetics

To determine the protein adsorption ability of the modified surfaces, bovine serum albumin (BSA) was selected as the model protein. A BSA adsorption kinetics assay was performed in 24-well tissue culture plates. Disk specimens (PEEK, PEEK-P, PEEK-P/pDA) were immersed in 0.5 ml bovine serum albumin (BSA) solution (pH = 7.35, 0.5 mg/ml) in each well under stirring at a constant rate of 100 rpm and at 37 °C. The effect of interaction time from 5 to 180 min on adsorption capacity was evaluated. Adsorbed protein amounts were determined through the decreasing BSA concentration within the samples using a BCA kit.

## Immobilization efficiency of IGF-1 or BMP-2

The amount of IGF-1 and BMP-2 immobilized onto the pDA-coated surface (PEEK-P/pDA) was evaluated by ELISA. Briefly, three different concentrations of IGF-1 or BMP-2 (10 ng/ml, 50 ng/ml, and 100 ng/ml) were prepared in phosphate-buffered saline (PBS). Next, each pDA-coated sample (PEEK-P/pDA) was immersed in different concentrations of IGF-1 or BMP-2 in 24-well tissue culture plates (1 ml/well) and incubated for 12 h at 4 °C. After incubation, the amount of immobilized growth factors on PEEK-P/pDA was determined based on the original and final solutions.

## Tensile mechanical properties

The tensile mechanical properties of the PEEK films (dimension 2 cm × 0.4 cm × 0.05 cm) after various treatments were evaluated by a universal mechanical testing machine (Instron 1121, UK) at room temperature. For each group, five duplicate specimens were tested and the tensile data were collected at a speed of 10 mm/min.

**Table 1** Abbreviations of samples

| Abbreviations | Samples |
|---|---|
| PEEK-P | PEEK immersed in concentrated sulfuric acid to fabricate a porous structure |
| PEEK-P/pDA | Porous PEEK (PEEK-P) decorated with pDA coating |
| PEEK-P/pDA/IGF1-1 | PEEK-P/pDA immobilized IGF-1 in 1 ml of 10 ng/ml IGF-1 solution |
| PEEK-P/pDA/IGF1-2 | PEEK-P/pDA immobilized IGF-1 in 1 ml of 50 ng/ml IGF-1 solution |
| PEEK-P/pDA/IGF1-3 | PEEK-P/pDA immobilized IGF-1 in 1 ml of 100 ng/ml IGF-1 solution |
| PEEK-P/pDA/BMP2-1 | PEEK-P/pDA immobilized BMP-2 in 1 ml of 10 ng/ml BMP-2 solution |
| PEEK-P/pDA/BMP2-2 | PEEK-P/pDA immobilized BMP-2 in 1 ml of 50 ng/ml BMP-2 solution |
| PEEK-P/pDA/BMP2-3 | PEEK-P/pDA immobilized BMP-2 in 1 ml of 100 ng/ml BMP-2 solution |
| PEEK-P/pDA/IGF1-BMP2 | PEEK-P/pDA immobilized growth factor in 1 ml solution containing 50 ng IGF-1 and 50 ng BMP-2 |

## In vitro studies

### Cell culture

In vitro experiments were performed to assess the ability of different samples to support MC3T3-E1 cell adhesion, spreading, proliferation, extracellular matrix secretion, and to further induce osteogenic differentiation. MC3T3-E1 cells have been frequently used for elucidating the responses of bone cells to biomaterials; these were cultivated in complete cell culture medium comprising Dulbecco's modified eagle medium (DMEM, Gibco) and 10% fetal bovine serum (FBS, Gibco) in a humidified atmosphere of 5% $CO_2$ at 37 °C. Before cell culture, all samples were sterilized with 75% alcohol for 40 min and rinsed thrice with sterile PBS. The cell culture medium was refreshed every other day.

### Cell adhesion and spreading

To investigate the effect of surface modification on cell adhesion and spreading, MC3T3-E1 cells were seeded on each sample in 24-well tissue culture plates at a density of $2 \times 10^4$ cells per well and incubated for 24 h. Afterward, the seeded samples were washed three times with PBS and fixed with 4% paraformaldehyde (PFA) at room temperature. The nuclei were stained with DAPI and examined by fluorescence microscopy (TE2000U, Nikon, JPN).

Cell spreading morphology was visualized by SEM. After culture for 24 h, the medium was removed, and the samples were rinsed with PBS and then fixed in 4% PFA solution for 30 min. The PFA solution was then removed, and the samples were washed thrice with PBS and dehydrated using a graded series of ethanol from 50% to 100% v/v (in water). The samples were kept in each solution for 30 min. Finally, the critically dried samples were sputtered with gold and examined under a scanning electron microscope (SEM).

### Cell proliferation

The CCK-8 assay was employed to determine the proliferation of MC3T3-E1 cells on the samples. MC3T3-E1 cells were seeded on each sample in 24-well tissue culture plates at a density of $2 \times 10^4$ cells/well and cultured for 1, 3, and 7 days. At the prescribed time points, 30 µl/well of CCK-8 was added to the medium. After 2 h of incubation, absorbance values at 450 nm were measured on a multifunctional micro-plate scanner (Tecan Infinite M200). Cell viability was calculated by the following equation.

$$\text{Cell viability} = \text{OD values}(\text{sample})/\text{OD values}\ (\text{pure PEEK})$$

### Extracellular matrix analysis

Extracellular matrix secretion was analyzed after MC3T3-E1 cells were cultured on the samples for 7 days and observed by SEM. The graded ethanol dehydration method was performed as described in the previous section.

### Alkaline Phosphate activity (ALP) assay

Cellular alkaline phosphatase activity (ALP) was measured using a previously established protocol [30]. Briefly, MC3T3-E1 cells were cultured on different substrates with an initial seeding density of $2 \times 10^4$ cells/well for 7 and 14 days, respectively. The medium in each well was carefully removed, and the cells were rinsed thrice with PBS at these time points. Afterward, the cells were lysed in RIPA buffer, followed by freezing and thawing repeatedly once or twice. Next, 50 µl of cell lysis solution was incubated with 200 µl of pNPP liquid substrate at 37 °C for 30 min. Absorbance at 405 nm was measured on a multifunction micro-plate scanner. The average absorbance values were used to reflect the level of ALP activity. The BCA assay kit was used to measure the total protein quantity for normalization.

### Mineralization of MC3T3-E1 cells

Alizarin red staining was used to detect the mineralization of MC3T3-E1 cells. The staining assay was performed as described in a previous study [31]. Briefly, MC3T3-E1 cells were cultured in different samples at a density of $2 \times 10^4$ cells/well for 14 and 21 days, respectively. At the prescribed time points, samples were washed three times in PBS and fixed in 4% PFA solution for 30 min. Then, 40 mM Alizarin red stain was added to the cell culture plates and incubated for 30 min. After washing three times in PBS, the different samples were observed under a light microscope. For the quantification of deposited minerals, 1 ml of 10% cetylpyridinium chloride

(CPC) solution was added to the ARS stained cell/samples for 1 h and the absorbance value of the solution was measured at 540 nm.

### Statistical analysis

All in vitro experiments were performed in three replicates.

All data were expressed as means ± standard deviations (SD). Statistically significant differences ($p$) among groups were measured using one-way analysis of variance (ANOVA) followed by Tukey's multiple-comparison analysis using SPSS 19.0 software. The differences were considered statistically significant at $p < 0.05$.

## Results and discussion

### Surface characterization

Figure 2a–c shows the SEM photographs acquired from PEEK-P, PEEK-P/pDA, and untreated PEEK samples. The surface of PEEK was relatively smooth (Fig. 2a) whereas a porous structure was observed in PEEK-P (Fig. 2b) and PEEK-P/pDA (Fig. 2c). The thickness of the porous layer of PEEK-P (Fig. 2e) and PEEK-P/pDA (Fig. 2f) was about 3.5 μm, indicating that about 3.5 μm of the PEEK surface was etched by the concentrated sulfuric acid. According to previous studies [32, 33], fabrication of a porous structure by concentrated sulfuric acid on the surface of PEEK might be due to the dissolution of PEEK, which was replaced by sulfonate PEEK. After washing with distilled water, the morphology of sulfonate PEEK was transformed from a swollen state to a solidified state. Solidified sulfonate PEEK would diffuse outward in the water to form a porous structure.

Comparison of the surface structure of PEEK-P and PEEK-P/pDA samples by SEM after pDA coating revealed similar surface morphology. However, the porous structure gained roughness on account of pDA coating. Furthermore, as shown in Fig. 3a, b, the size distribution of most pores on PEEK-P and PEEK-P/pDA was between 0.24 and 0.74 μm according to the analysis using Image J software. Thus, pore size was not obviously influenced by pDA coating.

The static water contact angles ($CA_{water}$) were evaluated to analyze the hydrophilicity of the modified surface. The measured water contact angles are summarized as a histogram in Fig. 2d, and the images of the water droplets on the samples are presented in the top right of Fig. 2a–c. Pure PEEK surfaces exhibited water contact angles of 96.35° ± 2.94°. Although the process of porous surface manufacture introduced hydrophilic $SO_3H$ groups on the surface, the water contact angle was significantly increased. PEEK-P ($CA_{water}$ = 105.83° ± 3.56°) samples were significantly more hydrophobic than the PEEK control. This implies that the surface morphology along with the porous structure plays a key role in increasing the surface hydrophobicity. After pDA modification, the water contact angle of PEEK-P/pDA (46.95° ± 3.75°) was significantly decreased. These results could be attributed to the pDA molecule layer, which reduced the interfacial energy between water and the pDA-modified PEEK-P [34].

XPS analysis was carried out to explore the chemical element changes in the samples at each step of the modification, and the results are presented in Fig. 4a–c. In wide spectra (Fig. 4a), the C1s and O1s peaks were very distinct. An inconspicuous peak was observed in the sulfur spectra (Fig. 4b) after immersion in concentrated sulfuric acid, but a corresponding peak was not detected in the wide spectra (Fig. 4a). The reason for this phenomenon might be related to the porous structure formation process mediated by concentrated sulfuric acid. Firstly, PEEK would be dissolved in concentrated sulfuric acid, followed by a sulfonation reaction. In this study, PEEK was immersed in concentrated sulfuric acid for a very short time (10 s), and so, introduction of the $SO_3H$ group on the surface was extremely rare and was scarcely observed.

After pDA coating, a new peak of N1 s at 400.16 eV appeared in the wide spectra of PEEK-P/pDA (Fig. 4a), and Fig. 4c is curve-fitted into two peak components with binding energies at about 399.1 eV and 402.5 eV ascribed to the introduction of amine groups by pDA coating. This confirmed that pDA was successfully coated onto the surface of PEEK-P.

### Protein adsorption

The effect of surface modification after pore fabrication and pDA coating on the protein adsorption ability was investigated, and the results are shown in Fig. 5. The maximum amount of BSA protein adsorbed on PEEK-P/pDA, PEEK-P, and PEEK was

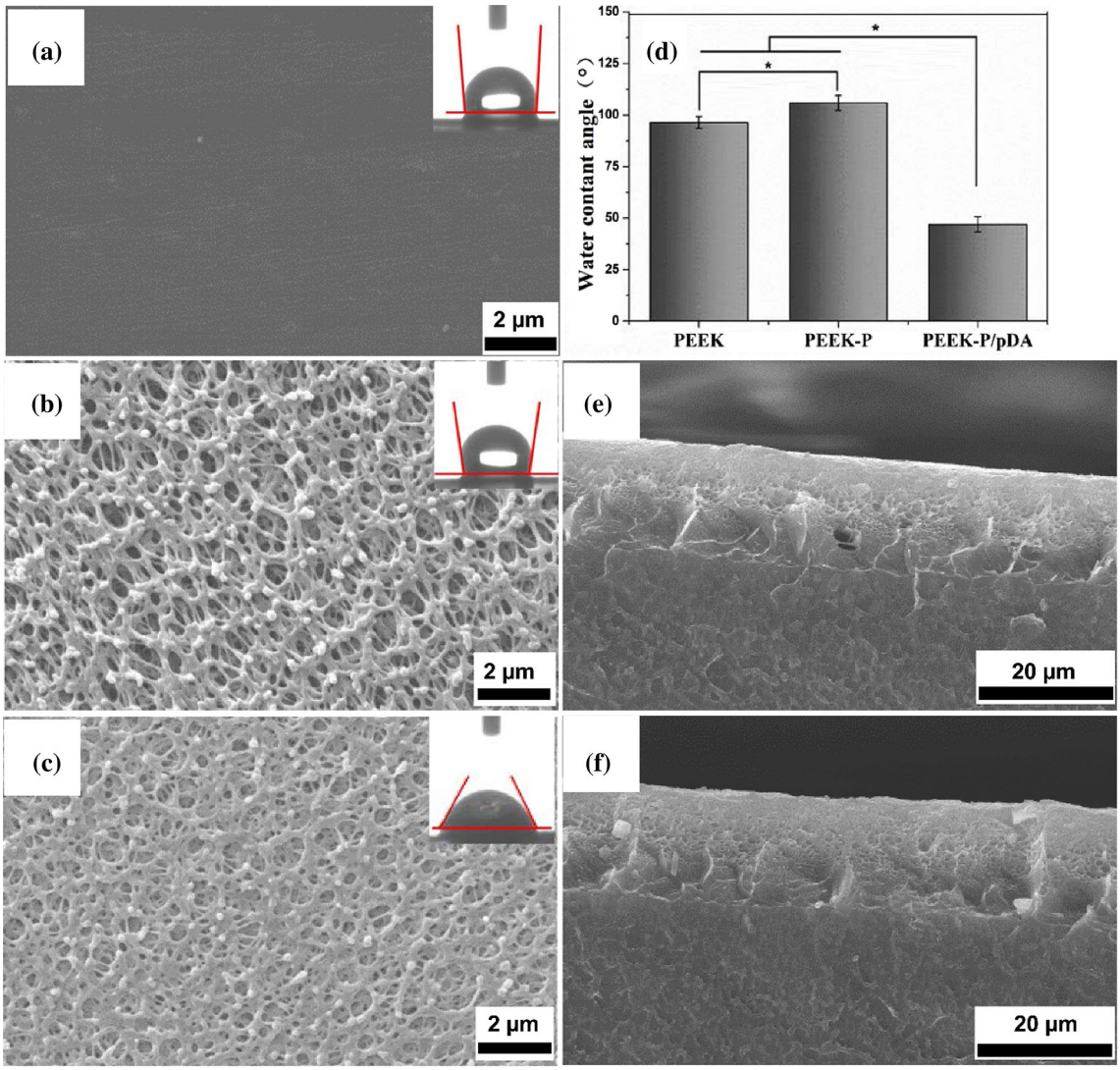


**Figure 2** SEM images showing the surface morphological features of PEEK control (**a**), PEEK-P (**b**), and PEEK-P/pDA (**c**) with typical water droplet images inserted in the top right and the water contact angles summarized in the histogram (**d**). Cross section of PEEK-P (**e**) and PEEK-P/pDA (**f**). $p < 0.05$, $n = 5$.

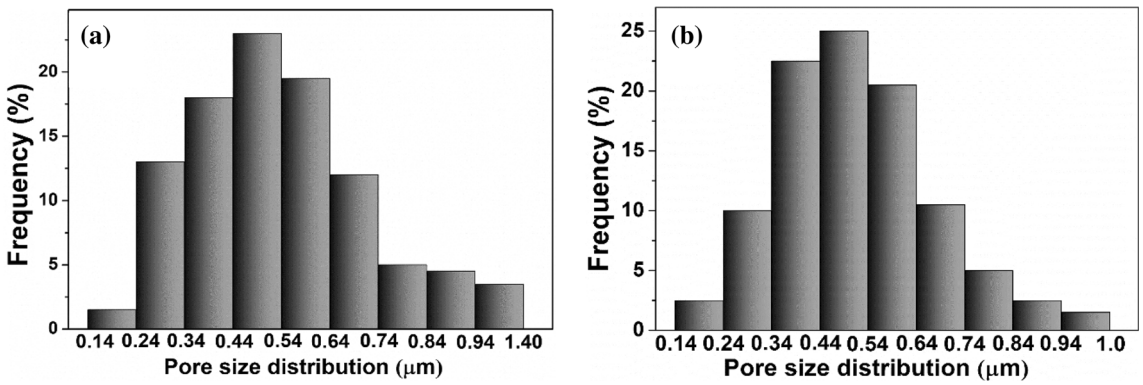


**Figure 3** Pore size frequency distribution of PEEK-P (**a**) and PEEK-P/pDA (**b**), measured using image J software.

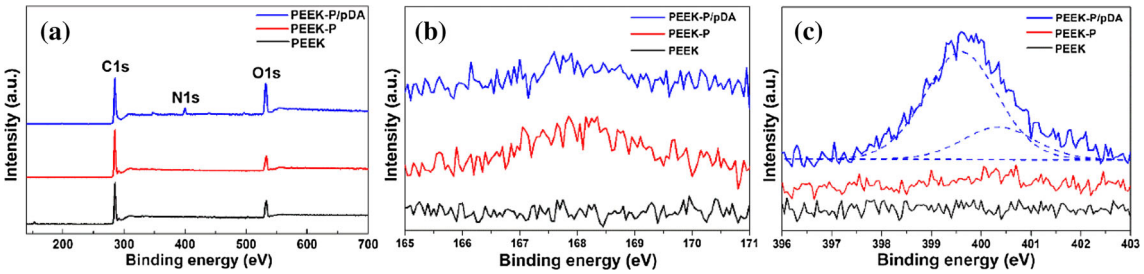


**Figure 4** XPS spectra of PEEK, PEEK-P, and PEEK-P/pDA samples. **a** Wide spectra. **b** S2*p* spectra. **c** N1*s* spectra.

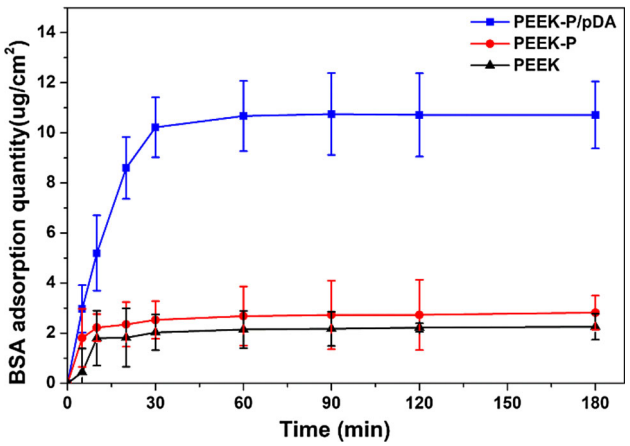


**Figure 5** Time-dependent BSA adsorption capacity of PEEK-P/pDA, PEEK-P, and PEEK samples from 5 min to 180 min. The concentration of BSA solution: 0.5 mg/ml, pH = 7.35, temperature: 37 °C.

10.716 μg/cm$^2$, 2.819 μg/cm$^2$, and 2.254 μg/cm$^2$, respectively. The results indicated that the protein adsorption ability of PEEK-P/pDA had improved greatly after pDA modification, with nearly 4.8 and 3.8 times the adsorption rates compared to those of PEEK and PEEK-P, respectively. Moreover, relatively faster adsorption rates were observed at the beginning (5 min) for pDA-modified PEEK, and the maximum adsorption capacity time (60 min) was longer than that of the control groups (20 min). Meanwhile, the protein adsorption capacity of PEEK-P was slightly higher than that of PEEK due to a higher specific surface area.

Generally, protein absorption onto materials mainly depends on physical absorption or chemical conjugation [35]. According to previous reports, during the self-polymerization process of pDA, catechol is first oxidized to quinone and further conjugated with amines, imidazole, or thiol groups to form ultrathin adhesive pDA films [36]. Thus, pDA allows surface immobilization of bioactive molecules, resulting in greater protein adsorption capacity for the pDA-modified PEEK. Simple physical adsorption of proteins on the PEEK and PEEK-P samples might occur due to weak interactions between the protein molecules and samples. The higher protein adsorption capacity of PEEK-P compared to normal PEEK might be a result of improved specific surface area after porous fabrication.

## Quantification of immobilized growth factors

Protein adsorption studies have revealed that pDA coating could significantly improve the adsorption ability of samples. In order to quantify the amount of immobilized growth factors on the surface of PEEK-P/pDA, ELISA was used in this study. Figure 6 shows that the quantity of immobilized IGF-1 on PEEK-P/pDA was 7.82 ng, 43.94 ng, and 86.54 ng corresponding to the treatment concentrations of

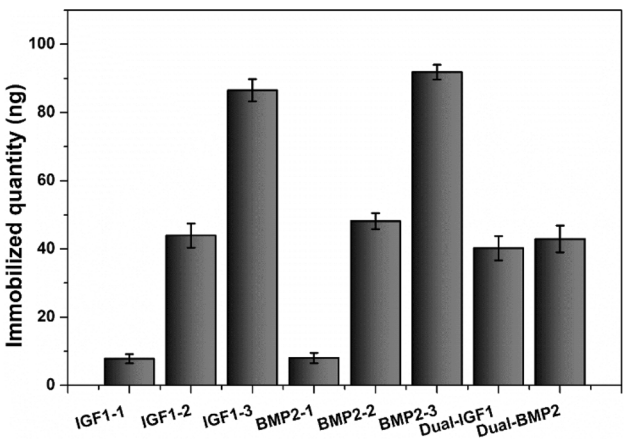


**Figure 6** The amount of IGF-1 or BMP-2 immobilized onto PEEK-P/pDA was evaluated by ELISA. IGF1-1, -2, -3 and BMP2-1, -2, -3 represent the treatment concentration of each growth factor solution at 10 ng/ml, 50 ng/ml and 100 ng/ml, respectively. Dual-IGF1 and dual-BMP2 represent the 50 ng/ml IGF-1 and 50 ng/ml BMP-2 combination groups.

10 ng/ml, 50 ng/ml, and 100 ng/ml, respectively. The amount of BMP-2 immobilized onto PEEK-P/pDA was 8.02 ng, 48.16 ng, and 91.86 ng corresponding to the treatment concentrations of 10 ng/ml, 50 ng/ml, and 100 ng/ml, respectively. This result indicated that the amount of immobilized IGF-1 or BMP-2 was enhanced by increasing the concentration of the growth factors. In the dual growth factor combination groups, the amount immobilized onto PEEK-P/pDA was 40.22 ng for IGF-1 and 42.92 ng for BMP-2, respectively. The result obtained in this study was consistent with that in our previous studies [37], showing that pDA coating is an efficient and simple method for conjugation of bioactive factors.

## Tensile mechanical properties

Figure 7 shows typical tensile stress–strain curves of pure PEEK and of samples with different treatments. The elastic modulus of all samples was calculated from the initial slopes of the tensile stress–strain curves to be about 3.6 GPa, demonstrating that the excellent bone-like elastic modulus property of PEEK materials could be preserved by this surface modification approach. However, the yield strength was decreased from 100.2 ± 3.8 MPa to 81.9 ± 1.3 MPa after fabricating the surface porous structure on PEEK films. A similar decrease in breaking elongation was also observed between pure PEEK and PEEK-P. The breaking elongation of pure PEEK was reduced from 226.9 ± 4.6% to 216.1 ± 2.5% after the porous fabricating process. According to the above results, the tensile mechanical property of PEEK materials was slightly decreased after the porous surface fabricating process. As described in previous section, PEEK would be dissolved in concentrated sulfuric acid during the porous fabricating process, consequently decreasing the yield strength and breaking elongation. The tensile mechanical property of various samples is summarized in Table 2. The results indicate that both pDA coating and the growth factor immobilization process would not influence the mechanical property of PEEK films.

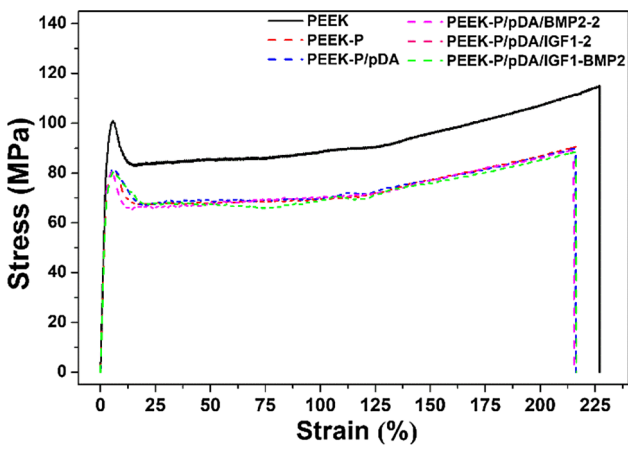


**Figure 7** The mechanical behavior of PEEK films after various treatments is shown as tensile stress–strain curves.

## Cell culture

### *Cell proliferation is influenced by the amount of IGF-1 and BMP-2*

We have previously reported that IGF-1 and BMP-2 can influence cell proliferation in a dose-dependent manner [40, 41]. Highly supra-physiological doses of growth factors dramatically increase the economic costs of treatments and result in undesired side effects due to their pleiotropic activity [42]. In this section, the influence of varying doses of IGF-1 or BMP-2 on MC3T3-E1 cell proliferation was examined in order to determine the suitable dosage for application in subsequent dual growth factor utilization experiments.

As shown in Fig. 8, after culture for 1 day, similar absorbance values were observed for all samples. After culturing for 3 and 7 days, low doses of IGF-1 (PEEK-P/pDA/IGF1-1) could significantly increase the cell proliferation of the samples. Furthermore, 50 ng/ml IGF-1 treatment (PEEK-P/pDA/IGF1-2) enhanced cell proliferation most effectively among the three IGF-1-loaded groups. However, as the IGF-1 concentration increased to 100 ng/ml, the OD values decreased, indicating that IGF-1 might promote the proliferation of MC3T3-E1 cells at low doses.

As shown in Fig. 8, OD values of 100 ng/ml BMP-2 treatment groups (PEEK-P/pDA/BMP2-3) were significantly lower than those of the low-dose treatment groups and PEEK-P/pDA at 3 and 7 days. The results demonstrated that excessively high doses of BMP-2 had a negative impact on cell proliferation. Cell proliferation was observed in the 10 ng/ml and 50 ng/ml BMP-2 treatment groups (PEEK-P/pDA/BMP2-1, PEEK-P/pDA/BMP2-2) at 1, 3, and 7 days and was higher on day 3, but showed no difference on day 7. According to previous studies [43], BMP-2 was one of the highly potent osteo-inductive factors

**Table 2** Tensile mechanical properties of pure PEEK and samples with different treatments show the mean elastic modulus (EM), yield strength (YS), and breaking elongation (%) for each group

| Samples | EM (GPa) | YS (MPa) | BE (%) |
|---|---|---|---|
| PEEK | 3.6 ± 0.17 | 100.2 ± 3.8 | 226.9 ± 4.6 |
| PEEK-P | 3.6 ± 0.20 | 81.8 ± 1.5 | 216.1 ± 2.5 |
| PEEK-P/pDA | 3.6 ± 0.23 | 81.5 ± 2.3 | 216.3 ± 4.2 |
| PEEK-P/pDA/BMP2-2 | 3.6 ± 0.26 | 80.7 ± 1.2 | 215.3 ± 3.6 |
| PEEK-P/pDA/IGF1-2 | 3.6 ± 0.16 | 80.6 ± 2.1 | 216.2 ± 5.2 |
| PEEK-P/pDA/IGF1-BMP2 | 3.6 ± 0.22 | 80.6 ± 3.2 | 216.2 ± 4.6 |
| Cortical bone [38] | 6 ~ 23 | | |
| Ti [39] | 116.3 ± 1.2 | | |

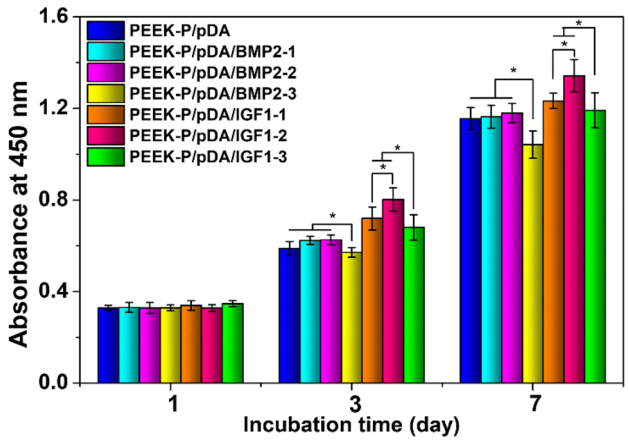


**Figure 8** CCK-8 assay showing the viability of MC3T3-E1 cells grown on samples loaded with different doses of IGF-1 or BMP-2 for 1, 3, and 7 days to determine the suitable dosage for the application in subsequent dual growth factor combining utilization experiments. The samples of PEEK-P/pDA were treated with 10 ng/ml, 50 ng/ml, and 100 ng/ml of IGF-1 or BMP-2 solution for 12 h. $p < 0.05$, $n = 3$.

with the main function of stimulating the differentiation of osteo-progenitor cells into mature osteoblasts. Possibly, the high doses of BMP-2 might induce excessive cell differentiation, which might negatively influence cell proliferation [44]. According to previous studies [13, 21], immobilization of BMP-2 onto biomaterials could significantly enhance the osteo-differentiation of cells. Moreover, the osteo-differentiation capacity of BMP-2 could be significantly enhanced with increasing treatment concentration. Thus, 50 ng/ml BMP-2 showed higher osteo-differentiation capacity among the three BMP-2-loaded groups and cell proliferation was not influenced at this treatment concentration. Therefore, the doses of 50 ng/ml IGF-1 and 50 ng/ml BMP-2 were applied in subsequent dual growth factor combining utilization experiments.

### *Cell adhesion and spreading*

In this section, MC3T3-E1 cell adhesion and spreading morphology were evaluated after 24-h incubation. In order to determine whether cells formed stable adhesions when grown on the samples, cell nuclei were fluorescently stained with DAPI (Fig. 9a–f) and SEM was used for directly observing the cell morphology on PEEK (Fig. 10a–f).

MC3T3-E1 adhered cell numbers on samples after 24-h incubation are shown in Fig. 9a–f. The number of adherent cells on PEEK-P was enhanced compared to that on the PEEK control, demonstrating that a porous structure could provide an attachment point and enhance MC3T3-E1 cell adhesion. This could also be detected from the images and the histogram (Fig. 9g). The number of adherent cells on the surface of PEEK-P/pDA was significantly increased compared to that on PEEK-P, indicating that cell adhesion was enhanced after pDA coating. Furthermore, after surface decoration with BMP-2 or IGF-1, cell adhesion was further improved compared to pure pDA coating. It is possible that the presence of BMP-2 and IGF-1 enhanced the cytocompatibility of samples and thus induced better cell adhesion [45, 46]. Interestingly, PEEK-P/pDA/BMP2-2 showed more MC3T3-E1 adherent cells compared to PEEK-P/pDA/IGF1-2, indicating that BMP-2 was more capable of improving cell adhesion than IGF-1. The number of attached cells on dual growth factor-loaded samples (PEEK-P/pDA/IGF1-BMP2) was substantially increased and presented statistically significant differences ($p < 0.05$) compared to the other groups. These results indicated that joint immobilization of IGF-1 and BMP-2 on PEEK substrates might have a greater influence than immobilization of IGF-1 or BMP-2 individually.

SEM images showed the spreading morphology of MC3T3-E1 cells after 24-h culture in different

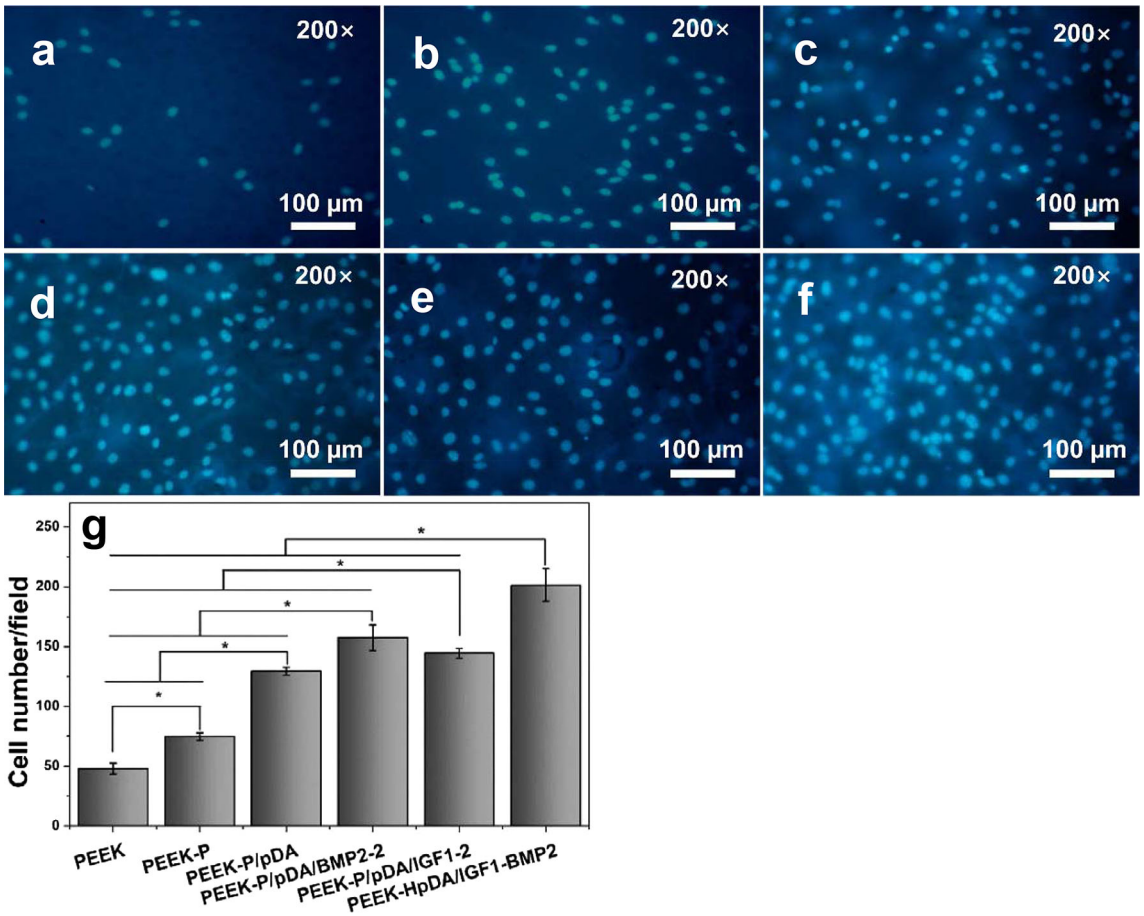


**Figure 9** Adhesion of MC3T3-E1 cells on various samples after 24-h incubation. Micrographs (**a**–**f**) of cell nuclei stained with DAPI observed under a fluorescence microscope. **g** Average numbers of MC3T3-E1 cells on different samples; three fields in total were counted for each group. $p < 0.05$, $n = 3$.

samples. As shown in Fig. 10a–f, the cell spreading morphology differed greatly on various sample surfaces. When observed closely, most of the MC3T3-E1 cells on the samples were found to be transformed from spheroid shape to thread spindles, whereas some still exhibited the pre-osteoblast morphology in the PEEK control. Cells growing on PEEK-P were partly adhered to the porous surface, and the unadhered parts were connected with the samples via pseudopods. After pDA coating, cells were spread to acquire their typical flat morphology and had formed thin lamellipodia extensions, indicating that cytocompatibility was significantly enhanced by pDA coating. The images of MC3T3-E1 cells grown on samples loaded with IGF-1 or BMP-2 showed the same trend of cell spreading, morphological elongation, and filopodia protrusions. Higher elongation ratios and more filopodia protrusions were detected in cells cultured on PEEK-P/pDA/BMP2-2 compared to those cultured on PEEK-P/pDA and PEEK-P/pDA/IGF1-2. The formation of distinct actin stress fibers and robust focal adhesions was indicative of cells forming stable attachments on PEEK-P/pDA, PEEK-P/pDA/BMP2-2, and PEEK-P/pDA/IGF1-2. Most obviously, a dense layer of cells grew partially on top of each other, featuring numerous filopodia and lamellipodia extensions as observed by SEM in PEEK-P/pDA/IGF1-BMP2, indicating that the cells had established strong attachment to the sample surface, with a distinct spreading morphology compared to those on other substrates.

### *Cell proliferation*

Cell proliferation on the IGF-1/BMP-2 dual-loaded samples and other samples was compared after culturing for 1, 3, and 7 days, and the results are shown in Fig. 11. After culturing for 3 and 7 days, PEEK-P

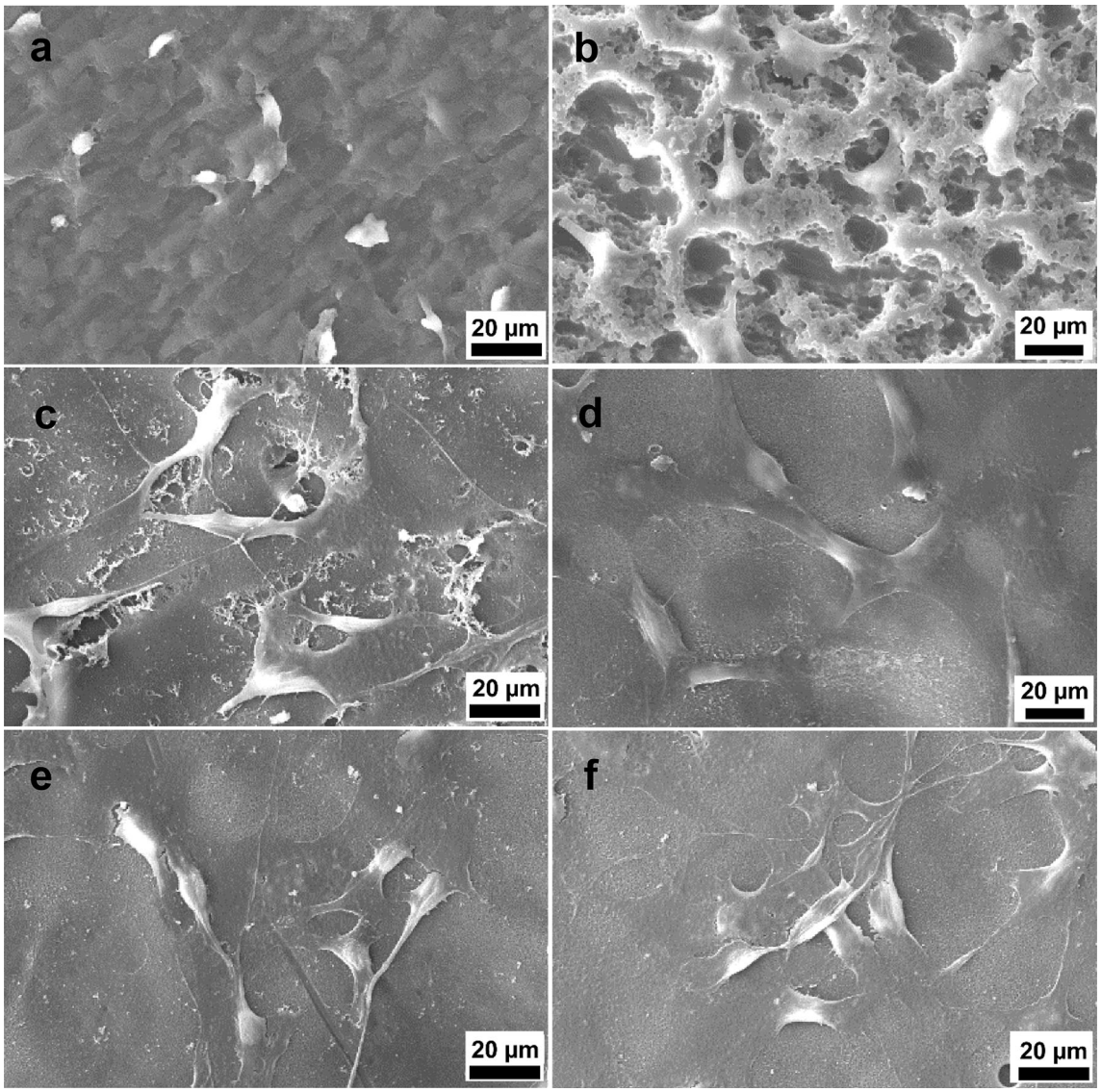


**Figure 10** SEM images of the morphology of MC3T3-E1 cells grown on PEEK (**a**), PEEK-P (**b**), PEEK-P/pDA (**c**), PEEK-P/pDA/BMP2-2 (**d**), PEEK-P/pDA/IGF1-2 (**e**), and PEEK-P/pDA/IGF1-BMP2 (**f**) after 24-h incubation.

exhibited higher cellular activity compared to PEEK. Previous studies have demonstrated that a porous structure is advantageous for cell adhesion and proliferation [47]. After pDA modification, the cell proliferation on PEEK-P/pDA was significantly enhanced at 3 and 7 days. Previous studies have reported [48] that pDA coating could significantly improve cell proliferation due to introduction of bioactive groups on the surface. Furthermore, the absorbance value in the PEEK-P/pDA/IGF1-2 group was higher than that in the PEEK-P/pDA/BMP2-2 and PEEK-P/pDA groups, indicating that IGF-1 could significantly enhance MC3T3-E1 cell proliferation. Notably, after culture for 3 and 7 days on diverse samples, the IGF-1- and BMP-2 dual-loaded samples (PEEK-P/pDA/IGF1-BMP2) enhanced cell proliferation most effectively compared to the other groups, indicating that the combination of IGF-1 and BMP-2 could significantly enhance cell proliferation compared to individual IGF-1 or BMP-2 treatments.

Cell adhesion, spreading morphology, and proliferation are known to be sensitive to material biocompatibility [49]. Cell adhesion is correlated with the cellular ability to survive and initiate proliferation on the substrate surface, with consequently increased cell spreading, increased cell survival, and cell cycling. Cell proliferation is closely correlated with the amount of new bone formation. Hence, better cell

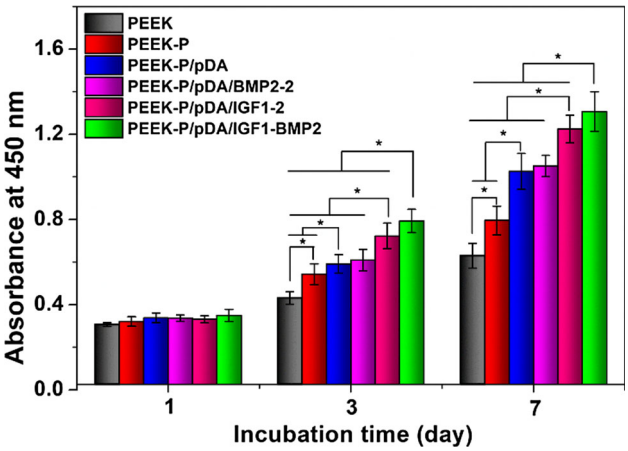


**Figure 11** Proliferation of MC3T3-E1 cells cultured on PEEK, PEEK-P, PEEK-P/pDA, PEEK-P/pDA/IGF1, PEEK-P/pDA/BMP2, and PEEK-P/pDA/IGF1-BMP2 for 1, 3, and 7 days was evaluated by CCK-8 assay. PEEK-P/pDA/IGF1-2 and PEEK-P/pDA/BMP2-2 were treated with 50 ng/ml IGF-1 or BMP-2 solution, respectively. The treatment solution of PEEK-P/pDA/IGF1-BMP2 included 50 ng IGF-1 and 50 ng BMP-2 per mL. $p < 0.05$, $n = 3$.

adhesion, spreading, and proliferation probably results in a larger amount of bone tissue around the implants and robust bone-implant bonding in vivo. These results on cell adhesion and spreading morphology were consistent with those of the CCK-8 assay and further support that samples loaded with the combination of IGF-1 and BMP-2 could provide a more cytocompatible environment for cellular responses.

### *Extracellular matrix (ECM)*

ECM proteins are the earliest products secreted by osteoblasts during cell adhesion and act as growth stimulators. The ECM plays an important role in signal transduction between cell and interface interactions and acts as a messenger. The ECM communicates with intracellular processes through the ECM–transmembrane–cytoskeleton network [50]. Formation of an efficient ECM is a pre-requisite for mineralization [51].

Thus, in this context, ECM secretion ofMC3T3-E1 cells was investigated by SEM after 7 days of culture. As shown in Fig. 12a–f, MC3T3-E1 cells attached on pure PEEK showed a spheroid shape and a modicum extracellular matrix with no clear evidence of intercellular connections. The cell number and diffusion area on the PEEK-P surface were higher than those on pure PEEK, with more ECM, and the cells showed a good spreading morphology on the porous structure. After pDA coating, a colony of cells embedded in a sheet of flimsy ECM and porous structure could be observed. MC3T3-E1 cells were healthily attached to the surface and multilayers of ECM covered almost the entire surface of PEEK-P/pDA/IGF1-2 and PEEK-P/pDA/BMP2-2 groups as shown in Fig. 12d and e, suggesting that IGF-1 and BMP-2 enhance MC3T3-E1 ECM secretion. In the dual growth factor-loaded group (PEEK-P/pDA/IGF1-BMP2), cells were almost buried in ECM and cell morphology was unclear; multilayer cell sheets covered the entire surface with elongated sheet like morphology, and evidences of intercellular connections were clearly observed.

### *Alkaline phosphate activity assay*

Alkaline phosphate activity (ALP) plays a crucial role during the differentiation stage and is recognized as an indicator of early interim-osteoblast differentiation [52]. Therefore, we evaluated the osteoblast differentiation of MC3T3-E1 cells cultured on different samples by measuring ALP activity. Figure 13 shows the ALP activities of MC3T3-E1 cells cultured on different substrates for 7 and 14 days. An increase in ALP activity was detected in cells grown on PEEK-P than on bare PEEK, indicating that the surface porous structure enhanced MC3T3-E1 cell differentiation during cell culture. After pDA coating, there were no significant differences in the ALP activities of MC3T3-E1 cells between PEEK-P and PEEK-P/pDA after 7 days in culture. However, after culturing for 14 days, the ALP activity of MC3T3-E1 cells cultured on the PEEK-P/pDA was slightly higher than that on PEEK-P. This might be because the pDA coating layer induced formation of bone-like apatite on the surface by soaking in simulated body fluid (SBF) by its capacity of attracting calcium ions; an apatite coating on the surface of PEEK-P/pDA provides an appropriate growth environment for the osteogenic differentiation of cells. Significantly higher ALP activities were detected in cells cultured on PEEK-P/pDA/BMP2-2 and PEEK-P/pDA/IGF1-2, indicating that BMP-2 or IGF-1 immobilized samples could effectively enhance MC3T3-E1 cells osteo-differentiation. Notably, the ALP levels of IGF-1 immobilized groups were lower than those of the BMP-2 immobilized groups (PEEK-P/pDA/BMP2-2), implying that BMP-

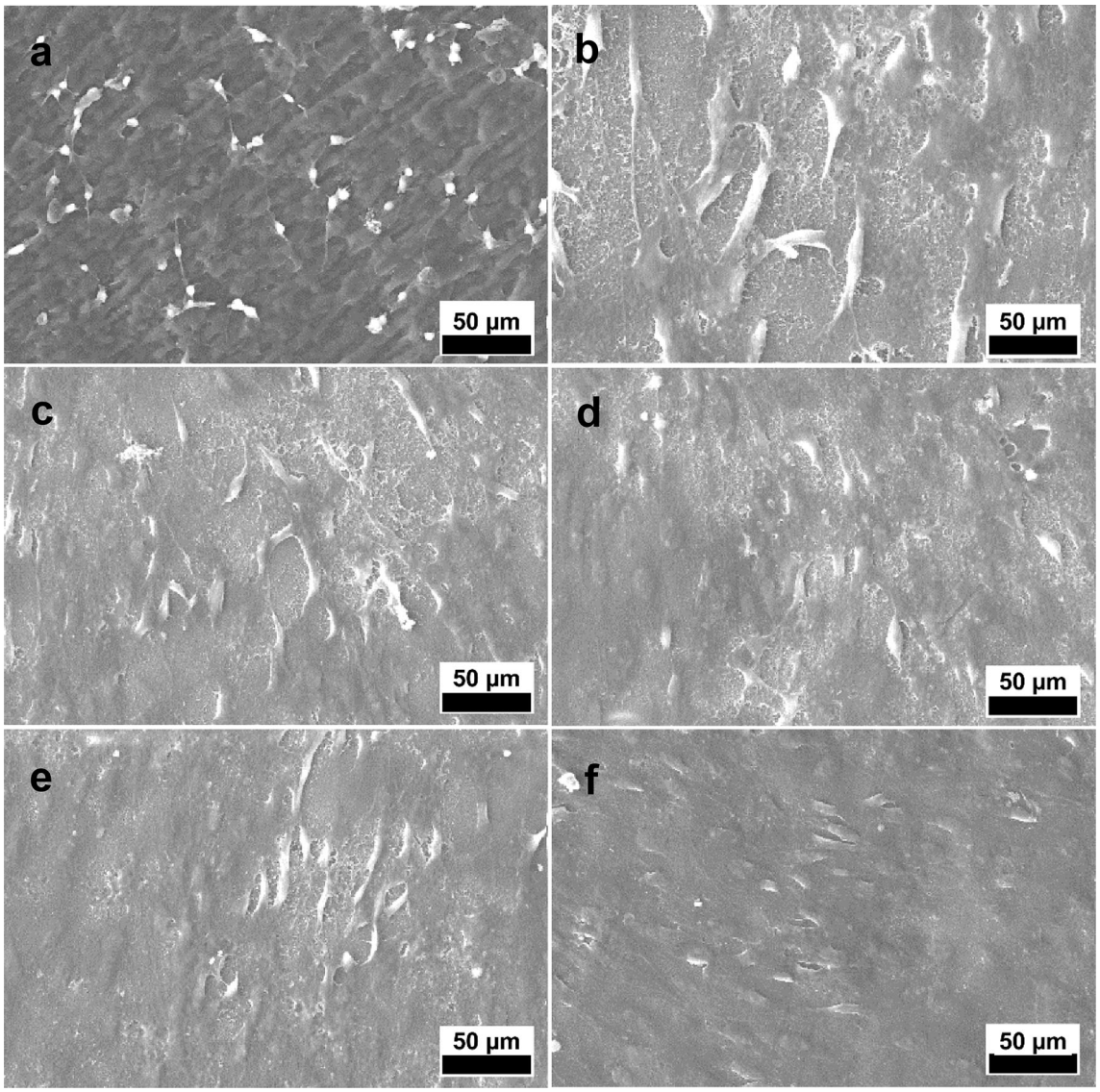


**Figure 12** SEM images of ECM secretion by MC3T3-E1 cells cultured on PEEK (**a**), PEEK-P (**b**), PEEK-P/pDA (**c**), PEEK-P/pDA/IGF1-2 (**d**), PEEK-P/pDA/BMP2-2 (**e**) and PEEK-P/pDA/IGF1-BMP2 (**f**) for 7 days.

2 had a greater capacity to improve osteogenic differentiation compared to IGF-1. The ALP levels of the dual immobilized IGF-1 and BMP-2 group (PEEK-P/pDA/IGF1-BMP2) were significantly increased compared to those of the individual BMP-2 group (PEEK-P/pDA/BMP2-2).

### *Mineralization*

Concomitantly, in order to evaluate the capacity of different samples to induce osteogenesis at late stages of differentiation, ARS staining was used to detect calcium deposition after incubation for 14 and 21 days. Figure 14a–f-1 shows the microscopic images after incubation for 14 days. ARS staining showed some mineral nodular deposits on PEEK-P (Fig. 14b-1) and PEEK-P/pDA (Fig. 14c-1), whereas almost no positive staining was observed on pure PEEK (Fig. 14a-1), demonstrating that the surface porous structure could facilitate calcium mineralization of MC3T3-E1 cells. Moreover, Fig. 14g indicates that the quantity of calcium minerals on PEEK-P/pDA was higher than that on PEEK-P, which corresponded with the results of our ALP activity study, indicating that pDA coating could enhance osteodifferentiation of MC3T3-E1 cells. After immobilization of IGF-1 or BMP-2, the samples of PEEK-P/pDA/IGF1-2 and PEEK-P/pDA/BMP2-2 showed

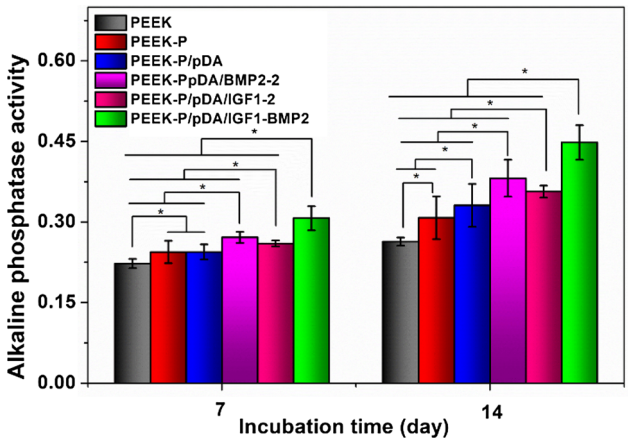


**Figure 13** Alkaline phosphatase activity (ALP) of MC3T3-E1 cells grown on different samples after incubation for 7 and 14 days, which was detected using the pNPP method. $p < 0.05$, $n = 3$.

more mineral nodules than those of PEEK-P/pDA. As shown in Fig. 14g, deposition of calcium minerals in PEEK-P/pDA/BMP2-2 groups was higher than that in the PEEK-P/pDA/IGF1-2 group, which might be attributed to the higher capacity of BMP-2 for improving osteogenic differentiation compared to that of IGF-1. Both calcium mineral staining (Fig. 14f-1) and quantitative analysis showed that the samples of PEEK-P/pDA/IGF1-BMP2 possessed the highest capacity to induce mineralization compared to the other groups.

ARS staining was also performed after 21-day incubation, and the resulting microscopic images are displayed in Fig. 14a–f-2. These showed more significant differences in the calcium minerals between each group after 21-day incubation. Among all groups, the most enhanced mineral nodules were observed in the PEEK-P/pDA/IGF1-BMP2, which corresponded with the 14-day analysis. The results demonstrated that the combination of BMP-2 and IGF-1 could significantly enhance cell differentiation compared to that observed with the immobilization of IGF-1 or BMP-2 alone.

Surface morphology plays an important role in the biocompatibility of biomaterials [9, 10, 53]. Porous structures are crucial for bioactive implants, because they directly affect protein adsorption, provide cell attachment points, bone integration capacity, and so on [54]. For this reason, concentrated sulfuric acid was utilized to fabricate a 3D network on the PEEK surface, which exhibited good bioactivity in vitro.

Hydrophilicity and protein adsorption capacity are an important factor for the function of stem cells as well as cell adhesion on biomaterials, and these parameters are crucial for bone tissue regeneration [55]. Hydrophilic surfaces can provide active sites for cellular attachment [56]. Protein adsorption influences cell adhesion by adsorption of key tissue protein adhesion molecules in vivo [57]. From the results of our study, surface modification via pDA coating enhanced the surface hydrophilicity and facilitated protein adsorption onto the implant surface. In vitro results showed that surface modification with pDA was an effective way to improve bioactivity and could provide an excellent microenvironment to promote cell attachment and proliferation.

In order to obtain a better bioactive surface, the combination of IGF-1 and BMP-2 was chosen in this study because the effect of BMP-2 alone on cell proliferation was unsatisfactory, and one of the important physiological functions of IGF-1 is to act as a factor promoting cell proliferation. Moreover, a previous study has shown that IGF-1 can promote BMP-2-mediated osteogenic differentiation [58]. The in vitro cell response analysis in our result shows that cell adhesion, spreading, proliferation, ECM secretion, and ALP activity are significantly enhanced on IGF-1/BMP-2 loaded PEEK compared to those with IGF-1 or BMP-2 alone. These results suggest that our surface bioactive modification can significantly enhance in vitro cell responses and possibly facilitate more robust bone/implant bonding in vivo.

## Conclusions

In this study, concentrated sulfuric acid was used to fabricate a surface porous structure on PEEK, followed by coating with pDA to improve hydrophilicity, cell attachment, and proliferation. Polydopamine coating could increase the number of binding sites for growth factors, which could effectively enhance BMP-2 and IGF-1 binding on the PEEK surface. Our in vitro results demonstrated that cell adhesion, spreading, proliferation, ECM secretion, and osteo-differentiation of MC3T3-E1 cells were enhanced after pDA coating. After immobilization of BMP-2 or IGF-1 (PEEK-P/pDA/BMP2-2, PEEK-P/pDA/IGF1-2), the samples exhibited excellent bioactivities with enhanced MC3T3-E1 cell function. As a surface modification for biomedical

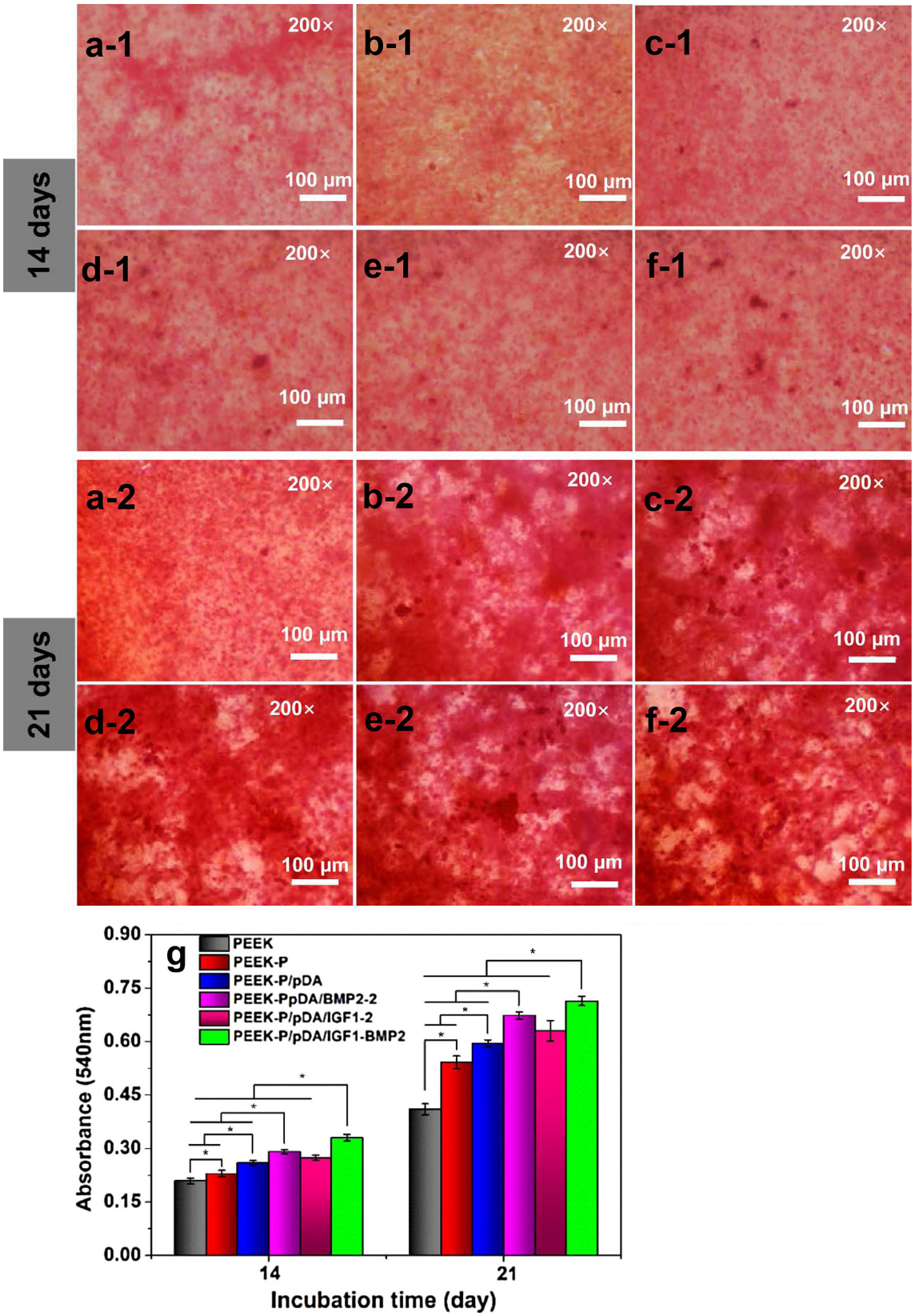
14 days
21 days
a-1
b-1
c-1
d-1
e-1
f-1
a-2
b-2
c-2
d-2
e-2
f-2
200×
100 μm
g
PEEK
PEEK-P
PEEK-P/pDA
PEEK-PpDA/BMP2-2
PEEK-P/pDA/IGF1-2
PEEK-P/pDA/IGF1-BMP2
Absorbance (540nm)
0.00
0.15
0.30
0.45
0.60
0.75
0.90
14
21
Incubation time (day)

◀**Figure 14** Alizarin red staining for mineralization of MC3T3-E1 cells cultured on various samples after 14-day incubation is shown in the images (**a**–**f**)-1 and the results after incubation for 21 days are shown in the images (**a**–**f**)-2. **g** Quantitative analysis of calcium minerals on different samples. $p < 0.05$, $n = 3$.

materials, we verified the in vitro cell response to the combined immobilization of BMP-2 and IGF-1 on the PEEK surface and compared the results obtained with those obtained after growth factors were immobilized individually on PEEK surface. The combination of IGF-1 and BMP-2 could facilitate cell attachment, spreading, proliferation, ECM secretion, and osteo-differentiation of MC3T3-E1 cells and significantly enhance the bioactivity of PEEK materials. Therefore, joint immobilization of IGF-1 and BMP-2 onto PEEK via pDA coating is a promising approach to prepare candidate materials for bone tissue engineering.

## Acknowledgements

This research was financially supported by the National Natural Science Foundation of China (Projects. 81672263, 51673186, and 51473164), the Program of Scientific Development of Jilin Province (20170520121JH and 20170520141JH), the joint funded program of Chinese Academy of Sciences and Japan Society for the Promotion of Science (GJHZ1519), and the Special Fund for Industrialization of Science and Technology Cooperation between Jilin Province and Chinese Academy of Sciences (2017SYHZ0021).

## Compliance with ethical standards

**Conflict of interest** The authors declare that they have no conflict of interest.

## References

[1] Yang J, Long T, He NF, Guo YP, Zhu ZA, Ke QF (2014) J Mater Chem B 2:6611. https://doi.org/10.1039/c4tb00940a

[2] Liu XY, Chu PK, Ding CX (2004) Mater Sci Eng R 47:49. https://doi.org/10.1016/j.mser.2004.11.001

[3] Thomas R, Maier S, Summer B (2004) Materialwiss Werkst 35:997. https://doi.org/10.1002/mawe.200400842

[4] Williams DF, Mcnamara A, Turner RM (1987) J Mater Sci Lett 6:188. https://doi.org/10.1007/BF01728981

[5] Katzer A, Marquardt H, Westendorf J, Wening JV, von Foerster G (2002) Biomaterials 23:1749. https://doi.org/10.1016/S0142-9612(01)00300-3

[6] Ma R, Tang TT (2014) Int J Mol Sci 15:5426. https://doi.org/10.3390/ijms15045426

[7] He RH, Lu YX, Ren JH et al (2017) Colloids Surface B 155:17. https://doi.org/10.1016/j.colsurfb.2017.03.055

[8] Deng Y, Yang L, Huang XB et al (2018) Macromol Biosci 18:1. https://doi.org/10.1002/mabi.201800028

[9] Ouyang L, Deng Y, Yang L et al (2018) Macromol Biosci. https://doi.org/10.1002/mabi.201800036

[10] Deng Y, Wei SC, Yang L, Yang WZ, Dargusch MS, Chen ZG (2018) Adv Funct Mater. https://doi.org/10.1002/adfm.201705546

[11] Wong KL, Wong CT, Liu WC et al (2009) Biomaterials 30:3810. https://doi.org/10.1016/j.biomaterials.2009.04.016

[12] Zhang YG, Zhu YJ, Chen F, Lu BQ (2017) Colloids Surface B 159:337. https://doi.org/10.1016/j.colsurfb.2017.07.093

[13] Lee SJ, Lee D, Yoon TR et al (2016) Acta Biomater 40:182. https://doi.org/10.1016/j.actbio.2016.02.006

[14] Chao C, Liu JD, Wang JT et al (2013) Acs Appl Mater Inter 5:10559. https://doi.org/10.1021/am4022973

[15] Giol ED, Schaubroeck D, Kersemans K, De Vos F, Van Vlierberghe S, Dubruel P (2015) Colloid Surface B 134:113. https://doi.org/10.1016/j.colsurfb.2015.04.035

[16] Tsai WB, Chen WT, Chien HW, Kuo WH, Wang MJ (2014) J Biomater Appl 28:837. https://doi.org/10.1177/0885328213483842

[17] Chen ZY, Zhang Z, Feng JT et al (2018) Acs Appl Mater Inter 10:11961. https://doi.org/10.1021/acsami.8b01547

[18] Zhou YZ, Cao Y, Liu W, Chu CH, Li QL (2012) Acs Appl Mater Inter 4:6900. https://doi.org/10.1021/am302041b

[19] Bessa PC, Casal M, Reis RL (2008) J Tissue Eng Regen M 2:81. https://doi.org/10.1002/term.74

[20] Liu YL, Enggist L, Kuffer AF, Buser D, Hunziker EB (2007) Biomaterials 28:5399. https://doi.org/10.1016/j.biomaterials.2007.08.024

[21] Song YH, Ju Y, Morita Y, Xu BY, Song GB (2014) Mat Sci Eng C-Mater 37:120. https://doi.org/10.1016/j.msec.2014.01.004

[22] Huang BL, Wu ZH, Ding S, Yuan Y, Liu CS (2018) Acta Biomater 71:184. https://doi.org/10.1016/j.actbio.2018.01.004

[23] Carreira AC, Lojudice FH, Halcsik E, Navarro RD, Sogayar MC, Granjeiro JM (2014) J Dent Res 93:335. https://doi.org/10.1177/0022034513518561

[24] Chen FM, Chen R, Wang XJ, Sun HH, Wu ZF (2009) Biomaterials 30:5215. https://doi.org/10.1016/j.biomaterials.2009.06.009

[25] Naskar D, Ghosh AK, Mandal M, Das P, Nandi SK, Kundu SC (2017) Biomaterials 136:67. https://doi.org/10.1016/j.biomaterials.2017.05.014

[26] Qiu T, Crane JL, Xie L, Xian LL, Xie H, Cao X (2018) Bone Res 6:1. https://doi.org/10.1038/s41413-017-0002-7

[27] Choi GH, Lee HJ, Lee SC (2014) Macromol Biosci 14:496. https://doi.org/10.1002/mabi.201300368

[28] Duruel T, Cakmak AS, Akman A, Nohutcu RM, Gumusderelioglu M (2017) Int J Biol Macromol 104:232. https://doi.org/10.1016/j.ijbiomac.2017.06.029

[29] Alas GR, Agarwal R, Collard DM, Garcia AJ (2017) Acta Biomater 59:108. https://doi.org/10.1016/j.actbio.2017.06.033

[30] Shi PJ, Liu M, Fan FJ, Yu CP, Lu WH, Du M (2018) Mat Sci Eng C-Mater 90:706. https://doi.org/10.1016/j.msec.2018.04.026

[31] Suhito IR, Han Y, Min J, Son H, Kim TH (2018) Biomaterials 154:223. https://doi.org/10.1016/j.biomaterials.2017.11.005

[32] Almasi D, Izman S, Assadian M, Ghanbari M, Kadir MRA (2014) Appl Surf Sci 314:1034. https://doi.org/10.1016/j.apsusc.2014.06.074

[33] Kurtz SM, Devine JN (2007) Biomaterials 28:4845. https://doi.org/10.1016/j.biomaterials.2007.07.013

[34] Liu CD, Liu C, Gao Y et al (2018) Adv Mater Interfaces. https://doi.org/10.1002/admi.201800003

[35] Xu YX, Han JM, Chai Y, Yuan SP, Lin H, Zhang XH (2018) Mat Sci Eng C-Mater 85:182. https://doi.org/10.1016/j.msec.2017.12.032

[36] Lee H, Dellatore SM, Miller WM, Messersmith PB (2007) Science 318:426. https://doi.org/10.1126/science.1147241

[37] Wang ZL, Chen L, Wang Y, Chen XS, Zhang PB (2016) Acs Appl Mater Inter 8:26559. https://doi.org/10.1021/acsami.6b08733

[38] Converse GL, Yue WM, Roeder RK (2007) Biomaterials 28:927. https://doi.org/10.1016/j.biomaterials.2006.10.031

[39] Wang LX, He S, Wu XM et al (2014) Biomaterials 35:6758. https://doi.org/10.1016/j.biomaterials.2014.04.085

[40] Gao TL, Zhang N, Wang ZL et al (2015) Macromol Biosci 15:1070. https://doi.org/10.1002/mabi.201500069

[41] Gao TL, Cui WW, Wang ZL et al (2016) RSC Adv 6:20202. https://doi.org/10.1039/c5ra27914c

[42] Pobloth AM, Duda GN, Giesecke MT, Dienelt A, Schwabe P (2017) J Tiss Eng Regen M 11:1514. https://doi.org/10.1002/term.2049

[43] Oryan A, Alidadi S, Moshiri A, Bigham-Sadegh A (2014) BioFactors 40:459. https://doi.org/10.1002/biof.1177

[44] Atluri K, Seabold D, Hong L, Elangovan S, Salem AK (2015) Mol Pharmaceut 12:3032. https://doi.org/10.1021/acs.molpharmaceut.5b00297

[45] Sun JC, Zhang YX, Li B, Gu Y, Chen L (2017) J Mater Chem B 5:8770. https://doi.org/10.1039/c7tb02043k

[46] Ito D, Kado T, Nagano-Takebe F, Hidaka T, Endo K, Furuichi Y (2015) J Biomed Mater Res A 103:3659. https://doi.org/10.1002/jbm.a.35476

[47] Zhao Y, Wong HM, Wang WH et al (2013) Biomaterials 34:9264. https://doi.org/10.1016/j.biomaterials.2013.08.071

[48] Li WY, Liu YS, Zhang P et al (2018) Acs Appl Mater Inter 10:5240. https://doi.org/10.1021/acsami.7b17620

[49] Zhao Y, Wu GS, Jiang J, Wong HM, Yeung KWK, Chu PK (2012) Corros Sci 59:360. https://doi.org/10.1016/j.corsci.2012.03.020

[50] Hagbard L, Cameron K, August P et al (2018) Philos T R Soc B. https://doi.org/10.1098/rstb.2017.0230

[51] Xiao Z, Camalier CE, Nagashima K et al (2007) J Cell Physiol 210:325. https://doi.org/10.1002/jcp.20826

[52] Park CS, Ha TH, Kim M et al (2018) Biosens Bioelectron 105:151. https://doi.org/10.1016/j.bios.2018.01.018

[53] Guan ZY, Chen YK, Wu CY, Wu SC, Yu JS, Chen HY (2018) J Mater Chem B 6:236. https://doi.org/10.1039/c7tb02758c

[54] Karageorgiou V, Kaplan D (2005) Biomaterials 26:5474. https://doi.org/10.1016/j.biomaterials.2005.02.002

[55] Liu W, Zhan JC, Su Y et al (2014) Colloids Surface B 113:101. https://doi.org/10.1016/j.colsurfb.2013.08.031

[56] Cheng CC, Lee DJ, Chen JK (2017) Acta Biomater 50:476. https://doi.org/10.1016/j.actbio.2016.12.031

[57] Xu Y, Han J, Chai Y, Yuan S, Lin H, Zhang X (2018) Mater Sci Eng C Mater Biol Appl 85:182. https://doi.org/10.1016/j.msec.2017.12.032

[58] Sluzalska KD, Liebisch G, Wilhelm J et al (2017) Sci Rep-Uk. https://doi.org/10.1038/s41598-017-14004-9